APPLIED AND ENVIRONMENTAL MICROBIOLOGY, Mar. 2007, p. 2001–2004 Vol. 73, No. 6
0099-2240/07/$08.00+0 doi:10.1128/AEM.02515-06

Biochemical Characterization of an L-Xylulose Reductase from *Neurospora crassa*▽†

Nikhil Nair[1] and Huimin Zhao[1,2,3,4]*

Departments of Chemical and Biomolecular Engineering[1] and Chemistry,[2] Center for Biophysics and Computational Biology,[3] and Institute for Genomic Biology,[4] University of Illinois at Urbana-Champaign, 600 S. Mathews Avenue, Urbana, Illinois 61801

Received 28 October 2006/Accepted 8 January 2007

An L-xylulose reductase identified from the genome sequence of the filamentous fungus *Neurospora crassa* was heterologously expressed in *Escherichia coli* as a His_6 tag fusion protein, purified, and characterized. The enzyme may be used in the production of xylitol from the major pentose components of hemicellulosic waste, D-xylose and L-arabinose.

L-Xylulose reductase (LXR; EC 1.1.1.10) is the third of five enzymes, in fungi, involved in the assimilation of L-arabinose into the pentose phosphate pathway (1). As a member of the short-chain dehydrogenase/reductase (SDR) superfamily, the catalytic action of LXR for the reduction of L-xylulose to xylitol requires a concomitant oxidization of a nicotinamide cofactor. With the exception of that from the yeast *Ambrosiozyma monospora*, all known LXRs are known to be strictly NADPH dependent (16). Although LXRs are also found in higher eukaryotes such as humans, guinea pigs, pigeons, and rats and catalyze the same reaction, their metabolic role is fundamentally different, realized in the glucuronic acid/uronate cycle of glucose metabolism (5, 15), and also the catalytic oxidation of α-dicarbonyl compounds (6, 12), rather than in L-arabinose metabolism.

Very few LXRs have been isolated and characterized to date; in fact, the identification of an LXR encoding gene in fungi was discovered only recently in *Trichoderma reesei* (*Hypocrea jecorina*) (13). In addition, LXRs have not found much commercial use, and their natural substrate, L-xylulose, is relatively expensive. We realize that the potential of LXR could be actualized in utilization of the pentose fraction hemicellulosic waste, which is primarily D-xylose and L-arabinose, for the production of xylitol, a pentitol sugar alternative with several favorable properties (7–11). Such a process would require concurrent utilization of three enzymes: a xylose reductase, an L-arabinitol-4-dehydrogenase, and an L-xylulose reductase. To the best of our knowledge, a fungal pathway for the co-utilization of D-xylose and L-arabinose to produce xylitol has never been attempted, either in vitro or in vivo. To implement such a strategy, a highly active and stable LXR from a fungal source needs to be identified, which has not yet been done. Here we report the identification, heterologous expression, purification, and characterization of a highly active and stable LXR from *Neurospora crassa*.

Gene identification. We postulated with the discovery of the highly catalytically efficient xylose reductase from *Neurospora crassa* (18) that the other enzymes involved the same L-arabinose utilization pathway may also be extremely active. Using the protein sequence of *T. reesei* LXR (GenBank accession no. AF375616.1) as a query for a BLASTP search (www.ncbi.nlm.nih.gov), the 271-amino-acid hypothetical protein NCU09041.1 in the *N. crassa* sequenced genome (3) was found as a putative LXR. A sequence alignment revealed a ~79% identity at the amino acid level with the search query. In addition, the protein has the conserved SDR catalytic triad of serine, tyrosine, and lysine (14). A BLAST search for homology with D-arabinitol dehydrogenases, enzymes with similar reaction substrate profiles, revealed ≤38% identity. These findings suggested that this hypothetical protein is most likely an LXR.

Cloning, heterologous expression, and purification. For experimental details, please see the supplemental material. PCR-amplified reverse-transcribed cDNA from L-arabinose-induced *N. crassa* 10333 showed a specific high-yield product of the expected gene size for *lxr*. This product was cloned into pET-28a(+) plasmid vector using NdeI and SacI restriction sites, which included an N-terminal His_6 tag via a thrombin-recognized linker sequence. The circularized plasmid was electroporated into *E. coli* BL21(DE3) and selected on kanamycin-supplemented LB plates.

After confirming soluble, active enzyme expression by sodium dodecyl sulfate-polyacrylamide gel electrophoresis (SDS-PAGE) analysis using cell lysates of isopropyl-β-D-thiogalactopyranoside (IPTG)-induced cultures, as well as by activity assay, the His_6-tagged LXR was purified by using single-step gravity immobilized metal affinity column chromatography. The protein concentration was determined by using the extinction coefficient as calculated by San Diego Supercomputer Center Biology Workbench (http://workbench.sdsc.edu) as 32,670 M^{-1} cm^{-1} at 280 nm. The enzyme purity was confirmed by SDS-PAGE analysis and stained with Coomassie brilliant blue. The final yield of tagged LXR was 18 mg (~60 mg/liter of culture) of >95% pure LXR with a molecular mass of ~30 kDa, which corresponds well to the calculated combined mass of ~31 kDa for the His_6-LXR (Fig. 1). Although the yield could be further improved by optimizing fermentation techniques, the acquired quantity and purity is sufficient for char-

* Corresponding author. Mailing address: Department of Chemical and Biomolecular Engineering, University of Illinois at Urbana-Champaign, 215 RAL, Box C3, 600 S. Mathews Ave., Urbana, IL 61801. Phone: (217) 333-2631. Fax: (217) 333-5052. E-mail: zhao5@uiuc.edu.

† Supplemental material for this article may be found at http://aem.asm.org/.

▽ Published ahead of print on 19 January 2007.

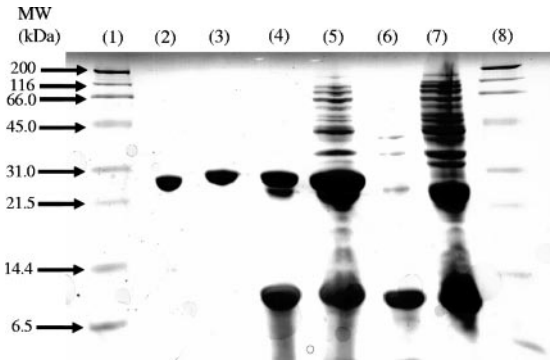

FIG. 1. SDS-PAGE analysis of purified, heterologously expressed *N. crassa* LXR. Lanes: 1 and 8, MW standard; 2, purified LXR after His_6 tag cleavage; 3, purified His_6-LXR fusion; 4 and 5, soluble and insoluble fractions, respectively, of cell lysate expressing His_6-LXR; 6 and 7, soluble and insoluble fractions, respectively, of cell lysate harboring empty plasmid (6). MW, molecular weight.

acterization purposes. The His_6 tag was cleaved by incubating the tagged LXR with thrombin (Fig. 1), and it was found that cleaving the tag restored ca. 16% of the activity (data not shown). Therefore, the untagged LXR was used for all further analysis.

Steady-state kinetics. Reaction kinetics were studied as for other NADP(H)-consuming oxidoreductases (18) by observing the initial change in absorbance at 340 nm using a UV-Vis spectrophotometer (as described in the supplemental material). All kinetic parameters for both forward and reverse reactions were determined at 25°C in 100 mM morpholinepropanesulfonic acid (MOPS; pH 7.0) and are summarized in Table 1. Purified *N. crassa* LXR had a strong preference for NADPH, displaying activity below the level of detection in the presence of NADH (see the description of high-performance liquid chromatography [HPLC] analysis for NADH acceptance below). The enzyme does not catalyze the reduction of L-arabinose, D-xylose, D-glucose, and D-galactose or the oxidation of L-arabinitol at detectable levels, which is consistent with other characterized LXRs (12, 13). Although the kinetic parameters for L-xylulose and D-xylulose could not be determined because the reaction velocity did not plateau in the range of concentrations tested, limited by cost of the expensive substrate, the K_m values seem to be unusually high. However, the enzyme displays the highest specific activity toward L-xylulose compared to any other substrate tested, including D-xylulose or D-ribulose (Table 1). LXRs have been known to have lower K_m values for D-ribulose than for L-xylulose (16). These data confirm that it is neither an D-arabinitol dehydrogenase nor an D-xylulose reductase but rather an LXR. The K_m values for all three pentulose substrates are at least 1 to 2 orders of magnitude higher than for any other characterized LXR, whereas the V_{max} is comparable to that of the yeast *A. monospora* but significantly higher than that of the fungus *T. reesei* (Table 2).

HPLC analysis for NADH acceptance. The acceptance of NADH as cofactor by *N. crassa* LXR was examined by HPLC. The separation of NAD^+ and NADH was carried out as described elsewhere (19). We set up 100-μl reaction mixtures consisting of 1 mM NADH and 10 mM D-ribulose in 100 mM MOPS (pH 7.0) and, after the addition of approximately 64.5 μg of enzyme, the reaction was allowed to proceed for 1 h at 25°C. Relative to the control reactions, this reaction yielded a significantly larger peak, with a retention time corresponding to authentic NAD^+ (see the supplemental material). This indicates that *N. crassa* LXR does accept NADH, although with a low average specific activity of 0.083 μmol/min/mg compared to 7.8 μmol/min/mg for NADPH as calculated for the same reactant concentrations.

Temperature dependence. The optimal temperature for catalysis was determined by assaying LXR activities at temperatures ranging from 15 to 60°C by using a recirculating water bath connected to the UV-Vis spectrophotometer with a jacketed cuvette holder. The data show the optimum reaction temperature to be approximately 37°C (Fig. 2A). At higher temperatures the enzyme rapidly inactivates, whereas at lower temperatures the rate decreases with temperature in accordance with Arrhenius' equation. The energy of activation for LXR was determined to be 19.8 ± 1.1 kJ/mol by fitting the data from 15 to 30°C to the Arrhenius equation. *N. crassa* LXR was found to be naturally stable, since it retained >85% activity after incubation at 25°C for over 6 h and >75% activity at 37°C after the same period of incubation (data not shown). Thermal inactivation was studied by incubating LXR in a heating block with a heated lid at 45°C in 100 mM MOPS (pH 7.0). Samples were removed at various times to detect residual activity at 25°C. The percent residual activity was plotted as a function of incubation time (Fig. 2B) and followed a first-order exponential decay with a half-life of about 13 min.

pH dependence. The effect of pH on LXR's activity was studied in constant-ionic-strength buffers to prevent the introduction of artifacts due to differing buffer components. For reduction, 2 mM D-ribulose and >200 μM NADPH in either acetate–2-(*N*-morpholino)ethanesulfonic acid (MES)–Tris buffer (pH 4.5 to 8.0) or MES–3-(cyclohexylamino)ethanesulfonic acid (CHES)–Tris buffer (pH 7.0 to 9.5) were used. Similarly, for oxidation 1,000 mM xylitol and 2 mM NADP in either acetate-MES-Tris buffer (pH 6.5 to 8.5) or Tris–CHES–3-(cyclohexylamino)-1-propanesulfonic acid (CAPS) buffer (pH 8.0 to 11.0) were used. The optimal pH was determined to be 7.0 for reduction and 9.0 for oxidation (Fig. 2C). The enzyme demonstrated a broad range of activity with >50% reductase activity between pH 4.5 and 8.5.

Determination of quaternary structure. To determine the quaternary structure, size-exclusion HPLC on a Bio-Sil SEC-250 column (300 by 7.8 mm) was performed by using an Agilent 1100 series HPLC system with 100 mM Na_2HPO_4, 150 mM NaCl, and

TABLE 1. Steady-state kinetics for *N. crassa* LXR[a]

Substrate	Mean ± SD		k_{cat}/K_m (mM^{-1} min^{-1})	Mean sp act (μmol/min/mg) ± SD
	K_m (mM)	k_{cat} (min^{-1})		
NADPH	0.0026 ± 0.0005	NA*	NA*	–
L-Xylulose	>275†	>6,000†		100 ± 19[b]
D-Xylulose	>275†	>1,500†		25 ± 1.2[b]
D-Ribulose	150 ± 12	7,140 ± 300	47.6	80 ± 1[b]
NADP	0.153 ± 0.025	NA*	NA*	–
Xylitol	1,239 ± 171	334 ± 25	0.269	–

[a] All assays performed in 100 mM MOPS (pH 7.0) at 25°C. *, the value of k_{cat} is limited by the choice of substrate. †, values could not be determined in the range of concentrations tested.
[b] At 275 mM substrate.

TABLE 2. Comparing properties of LXRs from fungi and yeast

Organism	Source or reference	Mean K_m (mM) ± SD			Mean K_m (μM) of NAD(P)H ± SD	Mean V_{max} (nkat mg^{-1}) ± SD			Assay conditions
		D-Ribulose	L-Xylulose	D-Xylulose		D-Ribulose	L-Xylulose	D-Xylulose	
N. crassa	This study	150 ± 12	>275	>275	2.6 ± 0.5	2,065 ± 79	>1,600	>400	25°C, pH 7.0
T. reesei	13	ND[b]	16 ± 3	ND	ND	ND	75 ± 10	ND	30°C, pH 7.0
A. niger	17	ND	17	ND	30	ND	ND	ND	ND
A. monospora[a]	16	4.7 ± 0.8	9.6 ± 0.7	ND	ND	2,700 ± 300	1,700 ± 300	ND	30°C, pH 7.0

[a] NADPH was a cofactor except NADH for *A. monospora*.
[b] ND, no data available.

10 mM NaN_3 (pH 6.8) as the mobile phase. A Bio-Rad standard was used to standardize the column's retention time with respect to molecular mass (see the supplemental material). The mass determined from the retention time was 62.2 kDa, close to a 58.2-kDa estimated mass for an LXR homodimer with a GlyHisSer linker remnant from the His_6 tag at the N terminus. Multimeric states are not uncommon, with several mammalian LXRs, including human, being tetrameric (2).

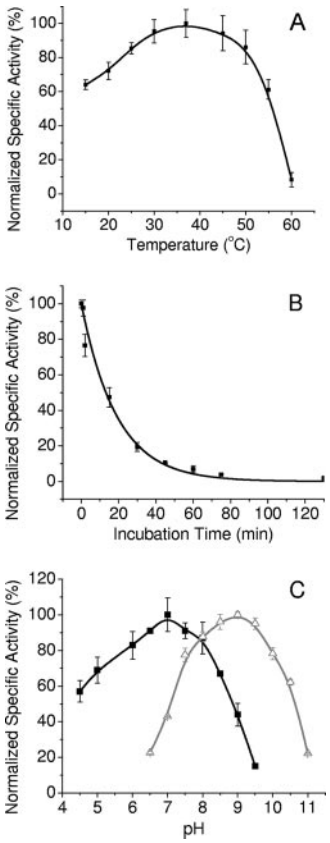

FIG. 2. (A) The temperature optimum for the reductase activity of *N. crassa* LXR was determined to be ~37°C when assayed between temperatures from 15 to 60°C. (B) Thermal inactivation of *N. crassa* LXR at 45°C. The heat inactivation followed first-order kinetics with a half-life of 12.9 min. (C) The pH optimum for the reductase activity (■) of *N. crassa* LXR was at 7.0 and at 9.0 for oxidase activity (△). The enzyme shows a broad range for activity with >50% reductase activity between pH 4.5 and 8.5.

Homology modeling. Using the coordinates (Protein Data Bank [PDB]; www.wwpdb.org) for the human LXR (PDB accession codes 1PR9 and 1WNT) (2) and the NADP-dependent mannitol 2-dehydrogenase from *Agaricus bisporus* (PDB accession code 1H5Q) (4), a homology model was created with the Molecular Operating Environment (MOE; Chemical Computing Group). Templates were chosen on the basis that the human LXR is the only LXR with a solved crystal structure, and mannitol 2-dehydrogenases are known to share high catalytic and sequence similarity with LXRs (13). The model was verified for consistency with known protein folds and allowed ϕ and ψ angles (see the supplemental material). Compared to the human LXR, the *N. crassa* LXR is longer by 14 amino acids in the N terminus. As can be seen from Fig. 3, the *N. crassa* LXR N terminus is modeled as an α-helix that is not present in the human LXR. The long distance of the N-terminal helix from the catalytic site explains why the addition of a linker and a His_6 tag does not significantly affect the catalytic efficiency of the protein. In addition, the *N. crassa* LXR is 27 amino acids longer, which would account for the longer loop regions. The catalytic triad Ser136, Tyr149, and Lys153 of human LXR have similar locations and orientations in the *N. crassa* LXR. The differing orientation of NADP in the active site is probably due to the steric effects between the bulky Tyr57 side chain and the adenine group of NADP in *N. crassa* LXR. In the human LXR, Ser37 is not likely to cause similar steric effects. The low levels of activity toward NADH can possibly be explained by the presence of hydrophobic Ala58 and Gly214 in the place of Arg39 and Ser185 in human LXR that stabilizes the 2′-phosphate group of NADPH. Although residues in the substrate binding site, other than the catalytic triad (Ser, Tyr, and Lys), are not strongly conserved between human and *N. crassa* LXR, they remain in general moderately to highly hydrophobic, with the exception of Asp220 in *N. crassa* LXR in place of Tyr191 (6), which would make the pocket more hydrophilic. However, the role of this residue seems unclear since it is conserved between the fungal LXRs, *N. crassa* and *T. reesei*, but not with the LXR from the yeast *A. monospora*, having a strongly hydrophobic Ile217 in the corresponding position.

In conclusion, we have identified and characterized a highly active LXR from *N. crassa* that can be heterologously expressed and purified with high yield in *E. coli*. The enzyme was characterized as stable and active over a wide range of temperatures and pH. Although it shows unusually high K_m values toward pentulose substrates, it displays one of the highest turnover numbers (k_{cat}) among characterized LXRs and may

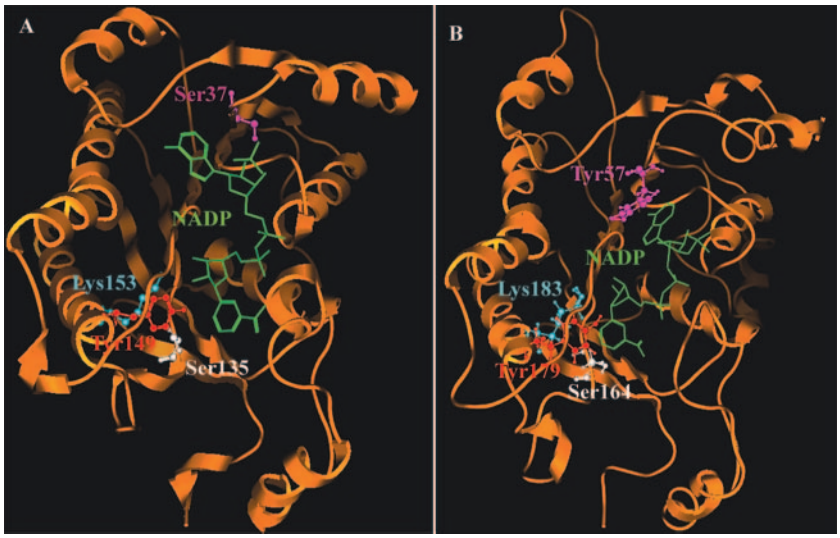

FIG. 3. Comparison of the crystal structure of human LXR (A) and homology model for *N. crassa* LXR with NADP (B). The catalytic triads (Ser, Tyr, and Lys) are shown and are approximately similar in position and orientation. Position of NADP differs in the two possibly because of Tyr57 in *N. crassa* LXR, offering steric hindrance to the adenine group of the cofactor. The longer N terminal is distant from the catalytic site, possibly accounting for minimal effect of the His_6 tag.

prove useful in the co-utilization of D-xylose and L-arabinose for the production of xylitol or ethanol.

Support for this research was provided by the Biotechnology Research and Development Consortium (project 2-4-121) and the Department of Chemical and Biomolecular Engineering at the University of Illinois at Urbana-Champaign.

Access to the Insight II and MOE programs was provided by The University of Illinois School of Chemical Sciences' Computer Application and Network Services. We thank Ryan Sullivan and Ryan Woodyer for help with the HPLC analyses and Hua Zhao for help in cloning and characterizing the L-xylulose reductase.

REFERENCES

1. **Chiang, C., and S. G. Knight.** 1960. A new pathway of pentose metabolism. Biochem. Biophys. Res. Commun. **3:**554–559.
2. **El-Kabbani, O., V. Carbone, C. Darmanin, S. Ishikura, and A. Hara.** 2005. Structure of the tetrameric form of human L-xylulose reductase: probing the inhibitor-binding site with molecular modeling and site-directed mutagenesis. Proteins **60:**424–432.
3. **Galagan, J. E., S. E. Calvo, K. A. Borkovich, E. U. Selker, N. D. Read, D. Jaffe, W. FitzHugh, L. J. Ma, S. Smirnov, S. Purcell, B. Rehman, T. Elkins, R. Engels, S. Wang, C. B. Nielsen, J. Butler, M. Endrizzi, D. Qui, P. Ianakiev, D. Bell-Pedersen, M. A. Nelson, M. Werner-Washburne, C. P. Selitrennikoff, J. A. Kinsey, E. L. Braun, A. Zelter, U. Schulte, G. O. Kothe, G. Jedd, W. Mewes, C. Staben, E. Marcotte, D. Greenberg, A. Roy, K. Foley, J. Naylor, N. Stange-Thomann, R. Barrett, S. Gnerre, M. Kamal, M. Kamvysselis, E. Mauceli, C. Bielke, S. Rudd, D. Frishman, S. Krystofova, C. Rasmussen, R. L. Metzenberg, D. D. Perkins, S. Kroken, C. Cogoni, G. Macino, D. Catcheside, W. Li, R. J. Pratt, S. A. Osmani, C. P. DeSouza, L. Glass, M. J. Orbach, J. A. Berglund, R. Voelker, O. Yarden, M. Plamann, S. Seiler, J. Dunlap, A. Radford, R. Aramayo, D. O. Natvig, L. A. Alex, G. Mannhaupt, D. J. Ebbole, M. Freitag, I. Paulsen, M. S. Sachs, E. S. Lander, C. Nusbaum, and B. Birren.** 2003. The genome sequence of the filamentous fungus *Neurospora crassa*. Nature **422:**859–868.
4. **Horer, S., J. Stoop, H. Mooibroek, U. Baumann, and J. Sassoon.** 2001. The crystallographic structure of the mannitol 2-dehydrogenase NADP+ binary complex from *Agaricus bisporus*. J. Biol. Chem. **276:**27555–27561.
5. **Hutcheson, R. M., V. H. Reynolds, and O. Touster.** 1956. The reduction of L-xylulose to xylitol by guinea pig liver mitochondria. J. Biol. Chem. **221:**697–709.
6. **Ishikura, S., T. Isaji, N. Usami, K. Kitahara, J. Nakagawa, and A. Hara.** 2001. Molecular cloning, expression and tissue distribution of hamster diacetyl reductase: identity with L-xylulose reductase. Chem. Biol. Interact. **130–132:**879–889.
7. **Kitchens, D. H.** 2005. Xylitol in the prevention of oral diseases. Spec. Care Dentist. **25:**140–144.
8. **Ly, K. A., P. Milgrom, and M. Rothen.** 2006. Xylitol, sweeteners, and dental caries. Pediatr. Dent. **28:**154–198.
9. **Maguire, A., and A. J. Rugg-Gunn.** 2003. Xylitol and caries prevention: is it a magic bullet? Br. Dent. J. **194:**429–436.
10. **Mattila, P. T., M. L. Knuuttila, and M. J. Svanberg.** 1998. Dietary xylitol supplementation prevents osteoporotic changes in streptozotocin-diabetic rats. Metabolism **47:**578–583.
11. **Mattila, P. T., M. J. Svanberg, P. Pokka, and M. L. Knuuttila.** 1998. Dietary xylitol protects against weakening of bone biomechanical properties in ovariectomized rats. J. Nutr. **128:**1811–1814.
12. **Nakagawa, J., S. Ishikura, J. Asami, T. Isaji, N. Usami, A. Hara, T. Sakurai, K. Tsuritani, K. Oda, M. Takahashi, M. Yoshimoto, N. Otsuka, and K. Kitamura.** 2002. Molecular characterization of mammalian dicarbonyl/L-xylulose reductase and its localization in kidney. J. Biol. Chem. **277:**17883–17891.
13. **Richard, P., M. Putkonen, R. Vaananen, J. Londesborough, and M. Penttila.** 2002. The missing link in the fungal L-arabinose catabolic pathway, identification of the L-xylulose reductase gene. Biochemistry **41:**6432–6437.
14. **Tanaka, N., T. Nonaka, K. T. Nakamura, and A. Hara.** 2001. SDR: structure, mechanism of action, and substrate recognition. Curr. Organic Chem. **5:**89–111.
15. **Touster, O., R. M. Hutcheson, and L. Rice.** 1955. The influence of D-glucuronolactone on the excretion of L-xylulose by humans and guinea pigs. J. Biol. Chem. **215:**677–684.
16. **Verho, R., M. Putkonen, J. Londesborough, M. Penttila, and P. Richard.** 2004. A novel NADH-linked L-xylulose reductase in the L-arabinose catabolic pathway of yeast. J. Biol. Chem. **279:**14746–14751.
17. **Witteveen, C. F. B., F. Weber, R. Busink, and J. Visser.** 1994. Isolation and characterization of two xylitol dehydrogenases from *Aspergillus niger*. Microbiology **140:**1679–1685.
18. **Woodyer, R., M. Simurdiak, W. A. van der Donk, and H. Zhao.** 2005. Heterologous expression, purification, and characterization of a highly active xylose reductase from *Neurospora crassa*. Appl. Environ. Microbiol. **71:**1642–1647.
19. **Woodyer, R., W. A. van der Donk, and H. Zhao.** 2003. Relaxing the nicotinamide cofactor specificity of phosphite dehydrogenase by rational design. Biochemistry **42:**11604–11614.